# Plaquette order in the $J_1$-$J_2$-$J_3$ model: Series expansion analysis

Marcelo Arlego*
*Departamento de Física, Universidad Nacional de La Plata, C.C. 67, 1900 La Plata, Argentina*

Wolfram Brenig
*Institut für Theoretische Physik, Technische Universität Braunschweig, 38106 Braunschweig, Germany*
(Received 19 August 2008; revised manuscript received 24 November 2008; published 17 December 2008)

Series expansion based on the flow equation method is employed to study the zero-temperature properties of the spin-1/2 $J_1$-$J_2$-$J_3$ antiferromagnet in two dimensions. Starting from the exact limit of decoupled plaquettes in a particular *generalized* $J_1$-$J_2$-$J_3$ model, we analyze the evolution of the ground-state energy and the elementary triplet excitations in powers of all three interplaquette couplings up to fifth order. We find that the plaquette phase remains stable over a wide range of exchange couplings and connects adiabatically up to the case of the plain $J_1$-$J_2$-$J_3$ model but not to the $J_1$-$J_2$ model at $J_3=0$. Besides confirming the existence of such a phase, recently predicted by Mambrini *et al.* [Phys. Rev. B **74**, 144422 (2006)], we estimate its extent by Dlog-Padé analysis of the critical lines that result from closure of the triplet gap.

DOI: 10.1103/PhysRevB.78.224415 PACS number(s): 75.10.Jm, 75.50.Ee, 75.40.−s, 78.30.−j

## I. INTRODUCTION

The study of quasi-two-dimensional (quasi-2D) materials with frustrated magnetic exchange interactions is a field of intense research. This research is driven by the quest for systems which may exhibit exotic magnetic phases instead of simple antiferromagnetic/ferromagnetic long-range order (AFM/FM LRO).[1] Prominent examples of such phases are spin liquids (SLs), with no ordering of any type, or valence bond states (VBSs). The latter may occur as solids (VBS) with no breaking of lattice symmetries but potentially other hidden order, such as, e.g., string ordering. Moreover valence bond crystals (VBC) are frequent, where lattice symmetries are directly broken in favor of, e.g., columnar or plaquette ordering.[1–3] Even for simple frustrated systems a quantitative understanding of the complete phase diagram is still lacking. The AFM spin-1/2 $J_1$-$J_2$ model on the square lattice is a paradigmatic case in this respect. This model corresponds to Fig. 1, for $J_1=J_0>0$, $J_2>0$, and $J_3=0$, where $J_1$ (and $J_0$) is the nearest-neighbor exchange interaction and frustration is induced by the next-nearest-neighbor exchange interaction $J_2$. Experimentally, $Li_2VOXO_4$ ($X$=Ge,Si), which has been discovered recently, is a promising candidate to realize the $J_1$-$J_2$ model in the range $J_2/J_1\sim 5-10$.[4,5] Two limiting cases of $J_1$-$J_2$ model are well understood. For $J_2=0$ and $J_1>0$, the system is the 2D Heisenberg AFM, which exhibits Néel LRO. In the opposite limit, $J_1/J_2\to 0$, the system turns into a set of two decoupled AFMs on the 2D $A$ and $B$ sublattices. These lock into a collinear state by the order-from-disorder effect due to the finite $J_2$. In the intermediate regime, $0.4\approx(J_2/J_1)_{c_1}<J_2/J_1<(J_2/J_1)_{c_2}\approx 0.6$, both the Néel and the collinear states are know to be unstable. Here, different approaches, including exact diagonalization (ED),[6–8] quantum Monte Carlo (QMC),[9,10] spin-wave (SW) theory,[11] large-$N$ expansion,[12,13] and series expansion (SE),[14–19] have confirmed that one or several quantum disordered phases with a singlet ground state and a gap to magnetic excitations may be present. The precise nature of the intermediate phase ($S$), however, is still controversial. In the simplest scenario, considering the existence of a single intermediate phase only, a plaquette VBC,[9] a columnar VBC,[12] and a SL (Ref. 10) have been proposed. Other studies suggest that the intermediate phase could be composed of two SL-like phases.[17]

The main purpose of this paper is to put the $J_1$-$J_2$ model into a broader perspective by considering an extended version, i.e., the $J_1$-$J_2$-$J_3$ model, which is depicted in Fig. 1 for $J_1=J_0$ and includes a third nearest-neighbor interaction $J_3$ (for clarity only some of the $J_3$ couplings are shown). Classically, the competing interactions $J_2/J_1$ and $J_3/J_1$ lead to four ordered phases of the $J_1$-$J_2$-$J_3$ model.[20–22] Among them, Néel and helicoidal phases, which are separated by a classical critical line $(J_2+2J_3)/J_1=1/2$ exist. The Néel phase remains rather stable against quantum fluctuations, although it has been conjectured that critical line, at $J_2=0$, should be shifted to $J_3/J_1>1/4$ once the quantum model is considered.[22]

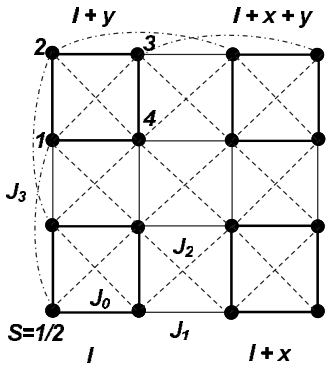


FIG. 1. The generalized $J_1$-$J_2$-$J_3$ model considered in this work. Solid circles represent spin-1/2 moments. Plaquettes (bold solid lines) are nonlocally coupled by nearest ($J_1$), next-nearest ($J_2$), and next-next-nearest ($J_3$) interactions, represented by thin solid, dashed, and dot-dashed lines, respectively. For clarity only some of the $J_3$ couplings are depicted. On each isolated plaquette, the couplings along the square edges are $J_0$ (bold solid lines) and across the diagonals $J_2$. At $J_1=J_0$ the $J_1$-$J_2$-$J_3$ model is recovered. $J_0$ couplings are set to unity hereafter.

 

The nature of the quantum phases in selected regions $J_1$, $J_2$, and $J_3$ has been considered recently by Mambrini *et al.*[23] By employing ED and diagonalization in a subset of short-range valence bond (SRVB) singlets (SRVB method) these authors have found evidence for a VBC-ordered, gapped plaquette phase in an extended region around the lines $(J_2+J_3)/J_1=1/2$ and $J_3 \geq J_2$. In this paper we will complement and extend these findings by performing SE analysis. In particular we will aim at a quantitative determination of the extension of the plaquette phase around the previously mentioned line by localizing the critical lines for a closure of the triplet gap.

Our strategy will be to analyze perturbatively the evolution of the ground state of a *generalized* version of the $J_1$-$J_2$-$J_3$ model. For this version $J_0 \neq J_1$. At $J_{1,3}=0$ and $J_2 \neq 0$ (only on those squares formed by the $J_0$ links) the generalized $J_1$-$J_2$-$J_3$ model shown in Fig. 1 exhibits a product state of disconnected bare four-spin "plaquettes." This will be the unperturbed ground state from which we start. The local $J_0$ couplings (bold lines) will be set to unity hereafter. Therefore at $J_1=1$ we recover the $J_1$-$J_2$-$J_3$ model (in units of $J_1$) from the generalized model. The Hamiltonian of generalized model is

$$H = H_0 + V, \quad H_0 = \sum_{\mathbf{l}} h_{0,\mathbf{l}}, \quad V = \sum_{\mathbf{l}} (V_{1,\mathbf{l}} + V_{2,\mathbf{l}} + V_{3,\mathbf{l}}), \tag{1}$$

where $h_{0,\mathbf{l}}$ refers to the local plaquette at site $\mathbf{l}$, given by

$$h_{0,\mathbf{l}} = [\mathbf{S}_1 \cdot \mathbf{S}_2 + \mathbf{S}_2 \cdot \mathbf{S}_3 + \mathbf{S}_3 \cdot \mathbf{S}_4 + \mathbf{S}_4 \cdot \mathbf{S}_1 + J_2(\mathbf{S}_1 \cdot \mathbf{S}_3 + \mathbf{S}_2 \cdot \mathbf{S}_4)]_{\mathbf{l}} = \frac{1}{2}[\mathbf{S}^2_{1234} - \mathbf{S}^2_{13} - \mathbf{S}^2_{24} + J_2(\mathbf{S}^2_{13} + \mathbf{S}^2_{24} - 3)]_{\mathbf{l}}, \tag{2}$$

where $\mathbf{S}_{1\ldots n}=\mathbf{S}_1+\ldots+\mathbf{S}_n$. $V_{1,\mathbf{l}}$, $V_{2,\mathbf{l}}$, and $V_{3,\mathbf{l}}$ in Eq. (1) represent the interplaquette coupling at site $\mathbf{l}$ via nearest ($J_1$), next-nearest ($J_2$), and next-next-nearest ($J_3$) interactions, respectively,

$$V_{1,\mathbf{l}} = J_1[\mathbf{S}_{3,\mathbf{l}} \cdot \mathbf{S}_{2,\mathbf{l}+\mathbf{x}} + \mathbf{S}_{4,\mathbf{l}} \cdot \mathbf{S}_{1,\mathbf{l}+\mathbf{x}} + \mathbf{S}_{2,\mathbf{l}} \cdot \mathbf{S}_{1,\mathbf{l}+\mathbf{y}} + \mathbf{S}_{3,\mathbf{l}} \cdot \mathbf{S}_{4,\mathbf{l}+\mathbf{y}}],$$

$$V_{2,\mathbf{l}} = J_2[\mathbf{S}_{4,\mathbf{l}} \cdot \mathbf{S}_{2,\mathbf{l}+\mathbf{x}} + \mathbf{S}_{3,\mathbf{l}} \cdot \mathbf{S}_{1,\mathbf{l}+\mathbf{x}} + \mathbf{S}_{2,\mathbf{l}} \cdot \mathbf{S}_{4,\mathbf{l}+\mathbf{y}} + \mathbf{S}_{3,\mathbf{l}} \cdot \mathbf{S}_{1,\mathbf{l}+\mathbf{y}} + \mathbf{S}_{3,\mathbf{l}} \cdot \mathbf{S}_{1,\mathbf{l}+\mathbf{x}+\mathbf{y}} + \mathbf{S}_{4,\mathbf{l}+\mathbf{y}} \cdot \mathbf{S}_{2,\mathbf{l}+\mathbf{x}}],$$

$$V_{3,\mathbf{l}} = J_3 \sum_{i=1}^{4} (\mathbf{S}_{i,\mathbf{l}} \cdot \mathbf{S}_{i,\mathbf{l}+\mathbf{x}} + \mathbf{S}_{i,\mathbf{l}} \cdot \mathbf{S}_{i,\mathbf{l}+\mathbf{y}}). \tag{3}$$

Table I shows the eigenstates of a local plaquette Hamiltonian, $h_{0,\mathbf{l}}$, in which each state is labeled by the ground-state energy: $e_0$, the total spin $S_{1234}$, and the spin along each diagonal $S_{13}$ and $S_{24}$.

From this table it follows that for $0 \leq J_2 < 1$ the ground state is $|\mathcal{S}_t\rangle$, i.e., a spin singlet along the plaquette and triplets along the diagonals. For $0 \leq J_2 < \frac{1}{2}$ the first-excited state is $|\mathcal{T}_t\rangle$, i.e., triplets along both the plaquette and the diagonals. At $J_2=1$ there is a crossover in the ground-state energy and thereafter the ground state is $|\mathcal{S}_s\rangle$, i.e., singlets along the plaquette and the diagonals. The other states are total triplets, $|\mathcal{T}_{ts}\rangle$ and $|\mathcal{T}_{st}\rangle$, consisting of a triplet on one of the diagonals and a triplet on the other one. Finally, there is a quintet state, $|\mathcal{Q}_t\rangle$.

TABLE I. Eigenstates of a local plaquette Hamiltonian, $h_{0,\mathbf{l}}$. Each state is labeled by the energy: $e_0$ and the quantum numbers $S_{1234}$, $S_{13}$, and $S_{24}$. Note that $J_0$ coupling has been set to unity.

| State | $q \equiv e_0+2$ | $S_{1234}$ | $S_{13}$ | $S_{24}$ |
|---|---|---|---|---|
| $\|\mathcal{S}_t\rangle$ | $\frac{1}{2}J_2$ | 0 | 1 | 1 |
| $\|\mathcal{T}_t\rangle$ | $\frac{1}{2}J_2+1$ | 1 | 1 | 1 |
| $\|\mathcal{S}_s\rangle$ | $-\frac{3}{2}J_2+2$ | 0 | 0 | 0 |
| $\|\mathcal{T}_{ts}\rangle$ | $-\frac{1}{2}J_2+2$ | 1 | 1 | 0 |
| $\|\mathcal{T}_{st}\rangle$ | $-\frac{1}{2}J_2+2$ | 1 | 0 | 1 |
| $\|\mathcal{Q}_t\rangle$ | $\frac{1}{2}J_2+3$ | 2 | 1 | 1 |

## II. SERIES EXPANSION BY CONTINUOUS UNITARY TRANSFORMATION

In this section we briefly describe the SE expansion in terms of $J_1$, $J_2$, and $J_3$. First, we rewrite the Hamiltonian [Eq. (1)] as

$$H = H_0(J_2=0) + J_2 O_2^0 + \sum_{i=1}^{3} \left( J_i \sum_{n=-N}^{N} O_i^n \right), \tag{4}$$

where $H_0$ has been split into the first two terms. The first one, $H_0(J_2=0)$, has a set of equally spaced energy levels (Table I). These are labeled with a *total particle-number* operator: $Q=\Sigma_{\mathbf{l}} q_{\mathbf{l}}(J_2=0)$. $Q=0$ corresponds to zero-particle states: $|\mathbf{0}\rangle \equiv \Pi_{\mathbf{l}}|\mathcal{S}_t\rangle_{\mathbf{l}}$. $Q=1$ sector corresponds to one-particle states: $|\mathbf{1}\rangle_{\mathbf{l}'} \equiv |\mathcal{T}_t\rangle_{\mathbf{l}'} \otimes \Pi_{\mathbf{l}\neq\mathbf{l}'}|\mathcal{S}_t\rangle_{\mathbf{l}}$, i.e., a local triplet at site $\mathbf{l}'$ created from the vacuum. $Q \geq 2$ sector of the spectrum is of multiparticle nature.

The second term in Eq. (4) refers to local contributions in $H_0$ proportional to $J_2$. The last three terms in the same equation (4) represent the interplaquette interactions, via $J_1$, $J_2$, and $J_3$, respectively. There, $O_i^n$ operators nonlocally create $(n \geq 0)$ and destroy $(n<0)$ quanta within the ladder spectrum of $H_0(J_2=0)$. The explicit tabulation of $O_i^n$ in this model shows that $N \leq 4$.[24]

It has been shown[25] that models of type (4) allow for SE by means of Wegner's continuous unitary transformation (CUT) method.[26] The basic idea is to map $H \rightarrow H_{\text{eff}}$, where

$$H_{\text{eff}} = H_0 + \sum_{k,m,l=1}^{\infty} C_{k,m,l} J_1^k J_2^m J_3^l. \tag{5}$$

The $C_{k,m,l}$ operators in Eq. (5) involve products of the $O_i^n$ operators of Eq. (4). However, as the main point and unlike in $H$, the effective Hamiltonian $H_{\text{eff}}$ is constructed to have a block-diagonal structure, where each block has a *fixed* number of particles $Q$ of $H_0(J_2=0)$. This is achieved order by order in the expansion. We refer to Ref. 25 for further details. In Secs. III–VI we will apply this technique to calculate the ground-state energy and the one-particle excitations.

### III. DISPERSION OF ONE-TRIPLET EXCITATIONS

In this section we evaluate the dispersion of one-triplet states for different values of the coupling constants, $J_1$, $J_2$, and $J_3$. To this end, it is necessary to diagonalize $H_{\text{eff}}$ in the $Q=1$ sector of $H_0(J_2=0)$, i.e., the subspace spanned by $|\mathbf{1}\rangle_\mathbf{l}$ states. $Q$ conservation implies that the sole action of $H_{\text{eff}}$ on the local triplet states refers to translation in real space; i.e.,

$$H_{\text{eff}}|\mathbf{1}\rangle_\mathbf{0} = \sum_\mathbf{l} c_\mathbf{l}|\mathbf{1}\rangle_\mathbf{l}, \tag{6}$$

where the $c_\mathbf{l}$'s are the hopping amplitudes of a local triplet from origin $\mathbf{0}$ to site $\mathbf{l}$. Due to the lattice translational invariance Eq. (6) can be diagonalized by Fourier transformation

$$E_\mathbf{1}(\mathbf{k}) = \sum_\mathbf{l} c_\mathbf{l} \exp(i\mathbf{k}\cdot\mathbf{l}). \tag{7}$$

From this, the dispersion $\omega(\mathbf{k})$ follows as

$$\omega(\mathbf{k}) = E_\mathbf{1}(\mathbf{k}) - E_\mathbf{0}, \tag{8}$$

where the ground-state energy, $E_\mathbf{0}$, is obtained by applying $Q$-conservation to the 0-particle sector; i.e., $E_\mathbf{0}=\langle 0|H_{\text{eff}}|0\rangle$. It is important to note that, even without an explicit discussion of this quantity, Eq. (8) requires a full calculation of the ground-state energy up to the same order as the hopping matrix elements.

By symmetry considerations not all the $c_\mathbf{l}$'s are independent, which leaves only a subset of them to be calculated. Usually, in CUT applications, the $c_\mathbf{l}$'s at O($n$) are obtained in the thermodynamic limit by considering finite clusters which are large enough to embed all the paths of length $n$ (Ref. 27) that connect origin $\mathbf{0}$ with site $\mathbf{l}$. In our model, due to the number of couplings considered and its dimensionality, this method becomes computationally very demanding. Alternatively, we have implemented a linked cluster approach, with subgraph subtraction to obtain the $c_\mathbf{l}$'s. We refer to Ref. 28 for technical details of this method. We have evaluated *analytic* expressions for the triplet dispersion, $\omega(\mathbf{k})$, keeping all three independent variables $J_1$, $J_2$, and $J_3$, i.e., without any parametrization, up to O(5).[29]

Figure 2 shows the dispersion obtained at O(5), as a function of wave vector $\mathbf{k}$, along high-symmetry directions and for different values of the couplings. We have chosen paths in the couplings space that show the instabilities of the plaquette phase associated with triplet softening; i.e., $\omega(\mathbf{k})=0$. We have selected two families of curves, parametrized according to $J_1$, $J_2=bJ_1$, and $J_3=cJ_1$, around $J_1=1$, the latter being the point where the $J_1$-$J_2$-$J_3$ model (in units of $J_1$) is recovered (see Fig. 1).

As shown in Fig. 2, triplet softening occurs at a critical wave vector of $\mathbf{k}_{c1}=(0,0)$ for the specific value of $(J_1,J_2,J_3)\approx(1,0.2,0.12)$, i.e., for relatively small values of $J_3$, as compared to $J_2$ (solid lines). Additionally, for larger values of $J_3$ a critical wave vector at $\mathbf{k}_{c2}=(\pi,\pi)$ (dashed lines) can be observed for the particular value of $(J_1,J_2,J_3)\approx(1.1,0.15,0.76)$ (dashed line). We have found no other values for critical wave vectors. *A priori* the critical wave vector does not determine a particular type of magnetic LRO beyond the critical couplings. This is because softening of

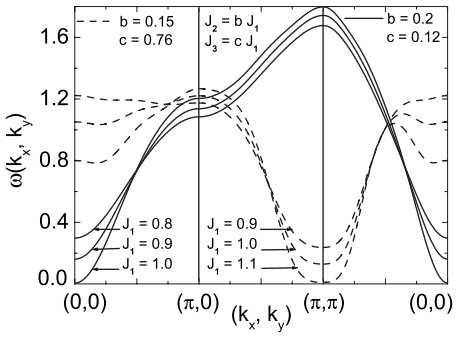


FIG. 2. Triplet dispersion $\omega(\mathbf{k})$ as a function of the wave vector $\mathbf{k}=(k_x,k_y)$ along the path $\mathbf{k}=(0,0)-(\pi,0)-(\pi,\pi)-(0,0)$. Two families of curves in coupling-constant space with parametrization $J_2=bJ_1$ and $J_3=cJ_1$ close to the actual $J_1$-$J_2$-$J_3$ model at $J_1=1$ have been selected to show triplet softening; i.e., $\omega(\mathbf{k})=0$. The instability at $\mathbf{k}_{c\mathbf{1}}=(0,0)$ occurs at small values of $J_3$, with respect to $J_1$ (solid lines). For larger values of $J_3$ the instability is at $\mathbf{k}_{c\mathbf{2}}=(\pi,\pi)$ (dashed lines).

the plaquette triplets at $\mathbf{k}_c$ does not uniquely fix a classical spin structure. Tentatively restricting the latter to helical order with pitch $\mathbf{q}$, simplifications arise. For example, $\mathbf{k}_{c1}=(0,0)$ is consistent with Néel order and $\mathbf{k}_{c2}=(\pi,\pi)$ on the lattice with spacing $2a\equiv 1$ of the plaquettes is consistent with $\mathbf{q}=(\pi/2,\pi/2)$ on the lattice with spacing $a\equiv 1$ of the spins. This pitch differs with simple classical analysis above the line $(J_2+2J_3)/J_1=1/2$.[20–22] The classical analysis however can be questioned since its ground-state energy is higher by roughly a factor of 2 as compared to the ground-state energy $E_g$ of the SE over all of the stability regions of the plaquette phase, *including* the instability lines of the SE. This leaves the large-$J_{2,3}$ region (see Fig. 5) an interesting open issue.[12,13] Figure 2 clarifies the type of critical points that have to be expected and is the first indication of the qualitative relevance of $J_3$ on the possible ground states of the model. To obtain a quantitative picture, the stability region of the plaquette phase in $J_1$-$J_2$-$J_3$ space will be studied in detail in Secs. IV–VI.

### IV. STABILITY OF THE PLAQUETTE PHASE

In this section we discuss the quantum critical lines, resulting from the closure of the plaquette triplet gap, which resembles second-order quantum phase transitions. This will give us a quantitative estimate of the stability region of the plaquette phase. In particular we are interested in a possible adiabatic connection of the isolated bare plaquette phase (with only local $J_2\neq 0$) up to the value of $J_1=1$. This analysis is shown in Fig. 3 which depicts the borders of the stability region projected onto $J_1$-$J_2$ plane, taking $J_3$ as parameter.

Figure 3 displays two families of critical lines, corresponding to the closure of the triplet gap $\omega(\mathbf{k}_c)=0$ for $\mathbf{k}_{c1}=(0,0)$ and $\mathbf{k}_{c2}=(\pi,\pi)$, with dotted and solid lines, respectively. First, it is obvious that independent of $J_2$ and $J_3$ the plaquette phase extends from the origin, $J_1=J_2=J_3=0$ (not shown in Fig. 3) up to $J_1\approx 0.55$ below which there are no

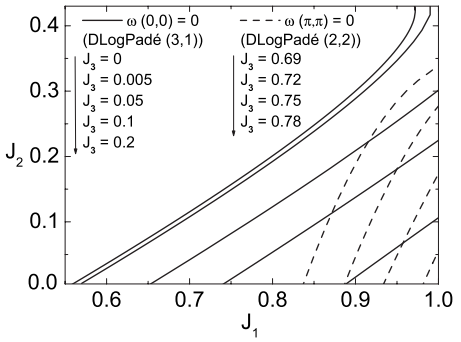


FIG. 3. Critical lines $[\omega(\mathbf{k}_c)=0]$ in $J_1$-$J_2$ plane and $J_3$ as parameter. Triplet softening occurs at $\mathbf{k}_{c1}=(0,0)$ and $\mathbf{k}_{c2}=(\pi,\pi)$, shown with solid and dashed lines, respectively. In all cases results from Dlog-Padé analysis are depicted. For $0\lesssim J_3\lesssim 0.4$, the instability at $\mathbf{k}_{c1}$ limits the plaquette phase, projected onto $J_1$-$J_2$ plane. But only for $J_3\gtrsim 0.05$ a plaquette phase appears in $J_1$-$J_2$-$J_3$ model (critical lines cross $J_1=1$). In particular, for $J_1=1$, $J_2$, and $J_3=0$, i.e., in the $J_1$-$J_2$ model, the plaquette phase is not present. For $0.7\lesssim J_3\lesssim 0.8$, the critical lines at $\mathbf{k}_{c2}$ limit the plaquette phase projected onto $J_1$-$J_2$ plane.

signals of triplet softening. Second, we focus on the $\omega(\mathbf{k}_{c1})=0$ instability. In the case of $J_3=0$, as can be observed from the figure, the critical line almost reaches but does not cross the line $J_1=1$. In other words, the $J_1$-$J_2$ model does not show a plaquette phase. This result is consistent with the previous SE analysis on $J_1$-$J_2$ model in Ref. 15. Third, we consider the simultaneous effect of $J_1$, $J_2$, and $J_3$. As can be observed in Fig. 3, increasing the values of $J_3$ enlarges the region of stability of the plaquette phase in the $J_1$-$J_2$ plane in terms of the critical line $\mathbf{k}_{c1}=(0,0)$ (solid lines). Most important, finite $J_3$ helps to stabilize the plaquette phase at $J_1=1$. In fact, already for $J_3\approx 0.05$ the critical line crosses $J_1=1$. For $J_3\approx 0.4$ the solid critical line merges with the lower right-hand corner of Fig. 3 and the plaquette phase extends over all of the $J_1$-$J_2$ planes shown. These results are consistent with Ref. 23.

Now we turn to the plaquette phase stability region, projected onto $J_1$-$J_2$ plane, limited by the critical lines $\omega(\mathbf{k}_{c2})=0$ (dotted lines in Fig. 3). We find a similar tendency as for $\mathbf{k}_{c2}$; i.e., the region of stability of the plaquette phase in the $J_1$-$J_2$ plane is enlarged by increasing $J_3$. In this case however the impact of $J_3$ is somewhat less significant as compared to $J_2$.

Technically, the critical lines of Fig. 3 have been obtained using Dlog-Padé analysis rather than the plain series. This is known to improve the accuracy of locating the critical points significantly. For details on this technique we refer the reader to the literature.[30] In order to work with single variable Dlog-Padés we have scanned the exchange coupling space by means of straight lines, parametrized according to $(J_1, J_2=bJ_1, J_3=cJ_1)$. For fixed values of $b$ and $c$ this amounts to a single variable, i.e., $J_1$.

To assess the impact of the Dlog-Padé analysis, we show its result for $\omega(\mathbf{k}_{c1})$, for a particular Dlog-Padé approximant and a case in which the triplet gap closes at $J_1=1$ (Fig. 4). A similar analysis has been done for all the critical lines calculated, including several Dlog-Padé approximants in each

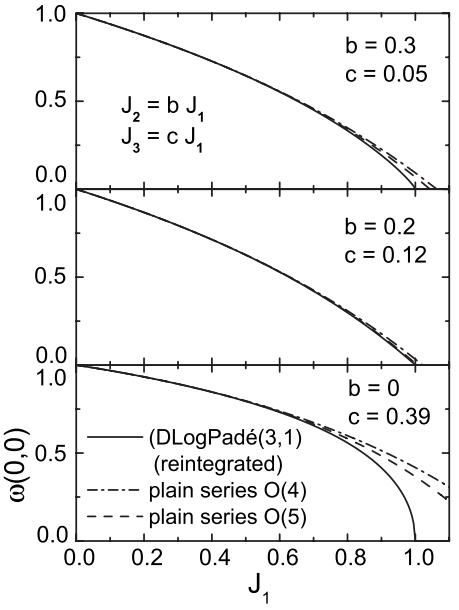


FIG. 4. Comparison between the triplet gap at $\mathbf{k}_c=(0,0)$ obtained by means of plain series and a particular Dlog-Padé approximant along selected straight-line paths in couplings space, for a case in which the triplet gap closes at $J_1=1$. Results from reintegrated Dlog-Padé (3,1), plain series at O(4) and O(5) are shown with solid, dot-dashed, and dashed lines, respectively. For $J_1\lesssim 0.5$ the agreement is very good in all cases. Closer to $J_1$-$J_2$-$J_3$ model, i.e., to $J_1=1$, clear differences between the Dlog-Padé and the plain series arise.

case. In this figure, the solid line refers to the reintegrated Dlog-Padé (3,1), and the dot-dashed and dashed lines show the plain series at O(4) and O(5), respectively. From there it is clear that for $J_1\lesssim 0.5$ the agreement between the reintegrated Dlog-Padé and the SE at O(4) and O(5) is very good. In fact, all plots are indistinguishable on the scale used. This provides a qualitative measure of the convergence of the series. For $J_1\gtrsim 0.5$ and closer to criticality (at $J_1=1$ in this case), however, we rely on the Dlog-Padé technique in order to describe the closure of the gap.

## V. PLAQUETTE PHASE AT $J_1=1$

Here we analyze the extent of the plaquette phase on the $J_2$-$J_3$ plane at $J_1=1$, i.e., for the actual $J_1$-$J_2$-$J_3$ model, written in units of $J_1$. As it was mentioned in Sec. I, ED calculations for $J_1$-$J_2$-$J_3$ model, using the complete Hilbert space and a restricted space of short-range dimer singlets, provide strong evidence for the existence of a plaquette phase around the line $J_2+J_3=1/2$ at $J_1=1$, in particular for $J_3\geq J_2$.[23] In this section, we will extend this study by specifying the extension of this phase as obtained from SE. To this end, we proceed as in Sec. IV; i.e., the critical lines are obtained by analyzing the closure of the triplet gap, i.e., solutions of $\omega(\mathbf{k})=0$.

In Fig. 5 we show the corresponding results. The lower and upper critical lines mark the triplet softening at $\mathbf{k}_{c1}$ and $\mathbf{k}_{c2}$, respectively, and enclose the region of a finite triplet gap. That is, this region refers to the plaquette phase, labeled

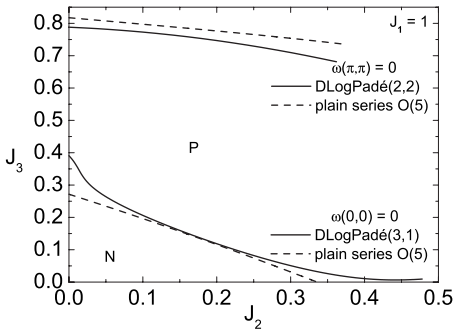


FIG. 5. Extension of the plaquette phase in $J_2$-$J_3$ plane at $J_1=1$ (actual $J_1$-$J_2$-$J_3$ model). The lower and upper critical lines represent the closure of the triplet gap at $\mathbf{k}_{c1}=(0,0)$ and $\mathbf{k}_{c2}=(\pi,\pi)$, respectively, which limit the plaquette phase (intermediate region labeled with P). Solid and dashed lines represent the results obtained employing Dlog-Padé approximants and plain series, respectively. The plaquette phase extends considerably around the straight line which connects ($J_2=0$, $J_3=0.5$) with ($J_2\approx J_3$, $J_3\approx 0.25$), previously studied in Ref. 23. Unlike the plain series, our Dlog-Padé analysis suggests that the plaquette phase is not present in $J_1$-$J_2$ model ($J_3=0$) for the parameters studied. However, for $0.35\lesssim J_2\lesssim 0.6$ the critical line is too close to $J_3=0$ to allow for definite statements at this order of SE.

as "P." In this figure, Dlog-Padé approximants are depicted by solid lines and the results obtained by employing the O(5) plain series by dashed lines. We note that the critical lines shown from Dlog-Padé approximants in Fig. 5 are consistent with the pairs of $(J_{2c},J_{3c})$ at $J_1=1$ shown in Fig. 3.

Although, as in Sec. IV, we base our results on the Dlog-Padé analysis, the agreement between the plain series and the Dlog-Padé approximants can be used to assess the convergence of the series. From Fig. 5, it is clear that the best agreement for the lower critical line is found in the intermediate region, i.e., where $0.1\lesssim J_{2,3}\lesssim 0.2$.

For the special case of $J_2=0$, i.e., for the pure $J_1$-$J_3$ model, it has been conjectured that the classical critical line to Néel phase at $J_3/J_1=0.25$ ($J_1=1$ in our case) should be shifted to larger values in the quantum model.[22] For all Dlog-Padés analyzed, our results confirm this conjecture, as, e.g., for the (3,1) Dlog-Padé approximant of the lower critical line shown in Fig. 5.

In conclusion we find that the plaquette phase extends considerably around the straight line of maximal frustration, connecting $J_2=0$ and $J_3=0.5$ with $J_2=J_3\simeq 0.25$, which was studied in Ref. 23. In particular, as it can be seen in Fig. 5, the upper critical line is rather far from the line of maximal frustration. Additionally, in the limiting case $J_3=0$, we remain with the $J_1$-$J_2$ model. For the latter, and as shown in the right lower corner of Fig. 5, and unlike the plain series, the Dlog-Padé analysis suggests that the critical line does not intersect the $J_2$ axis. That is, we find no stability in the plaquette phase. This is in agreement with the SE results of Ref. 15. Yet, the proximity between the critical line and the $J_2$ axis calls for caution on this finding with respect to the convergence of the SE in this parameter range.

## VI. CONCLUSIONS

To summarize, using series expansion, based on flow equations we have analyzed the zero-temperature properties of the 2D spin-1/2 $J_1$-$J_2$-$J_3$ AFM. Starting from the limit of decoupled plaquettes of a generalized $J_1$-$J_2$-$J_3$ model we have evaluated three-parameter series up to O(5) in the interplaquette exchange couplings $J_1$, $J_2$, and $J_3$ for the ground-state energy and for the triplet dispersion.

We find a rather large range of $J_{1,2,3}$ couplings which adiabatically connects to the state of isolated plaquettes and hosts a plaquette phase which is stable against second-order quantum phase transitions into magnetic states. Our findings corroborate and enhance related predictions of Mambrini *et al.*[23] on the location of a stable plaquette phase at $J_1=1$.

For the particular case of the $J_1$-$J_2$ model at $J_3=0$, and consistently with results obtained in Ref. 15, our calculation predicts that the plaquette phase is not stable in the parameter range which we have investigated. However, higher-order series expansions seem very desirable to render such results more reliable. In particular, from our series we are reluctant to draw any definite conclusions about the controversial region $J_3=0$ and $0.4\lesssim J_2\lesssim 0.6$.

Finally, we emphasize that our analysis has been focused on the stability of the plaquette phase with respect to second-order transitions driven by one-particle (triplet) excitations. Further instabilities, such as first-order transitions or level crossings of excited states, other than elementary triplets, could give rise to further reduction in the plaquette regime and have not been considered here. Along this line, the two-particle sector, which includes singlet excitations, may play a role that can be analyzed using our SE technique. This deserves future investigation.

## ACKNOWLEDGMENTS

We would like to thank D. Poilblanc and A. Läuchli for helpful comments. We also acknowledge support from the Rechenzentrum of the TU Braunschweig and IFLP of the UNLP where parts of the numerical computations have been performed on CFGAUSS and Bose Clusters, respectively. This research was supported in part by DFG, Germany through Grant No. BR 1084/4-1; CONICET, Argentina through Grant No. PIP 5037; and ANCYPT, Argentina through Grant No. PICT 20350.

*m.arlego@fisica.unlp.edu.ar

[1] G. Misguich and C. Lhuillier, in *Frustrated Spin Systems*, edited by H. T. Diep (World Scientific, Singapore, 2005).

[2] J. Richter, J. Schulenburg, and A. Honecker, in *Quantum Magnetism*, Lecture Notes in Physics Vol. 645, edited by U. Schollwök, J. Richter, D. J. J. Farnell, and R. F. Bishop (Springer-Verlag, Berlin, 2004).

[3] F. Alet, A. M. Walczak, and M. P. Fisher, Physica A **369**, 122

(2006).
[4] R. Melzi, P. Carretta, A. Lascialfari, M. Mambrini, M. Troyer, P. Millet, and F. Mila, Phys. Rev. Lett. **85**, 1318 (2000).
[5] H. Rosner, R. R. P. Singh, W. H. Zheng, J. Oitmaa, S. L. Drechsler, and W. E. Pickett, Phys. Rev. Lett. **88**, 186405 (2002).
[6] E. Dagotto and A. Moreo, Phys. Rev. Lett. **63**, 2148 (1989).
[7] D. Poilblanc, E. Gagliano, S. Bacci, and E. Dagotto, Phys. Rev. B **43**, 10970 (1991).
[8] H. J. Schulz, T. Ziman, and D. Poilblanc, J. Phys. I **6**, 675 (1996).
[9] L. Capriotti and S. Sorella, Phys. Rev. Lett. **84**, 3173 (2000).
[10] L. Capriotti, F. Becca, A. Parola, and S. Sorella, Phys. Rev. Lett. **87**, 097201 (2001).
[11] P. Chandra and B. Doucot, Phys. Rev. B **38**, 9335 (1988).
[12] N. Read and S. Sachdev, Phys. Rev. Lett. **62**, 1694 (1989).
[13] S. Sachdev and N. Read, Int. J. Mod. Phys. B **5**, 219 (1991).
[14] M. P. Gelfand, Phys. Rev. B **42**, 8206 (1990).
[15] R. R. P. Singh, Z. Weihong, C. J. Hamer, and J. Oitmaa, Phys. Rev. B **60**, 7278 (1999).
[16] V. N. Kotov, J. Oitmaa, O. P. Sushkov, and Z. Weihong, Philos. Mag. A **80**, 1483 (2000).
[17] O. P. Sushkov, J. Oitmaa, and Z. Weihong, Phys. Rev. B **63**, 104420 (2001).
[18] O. P. Sushkov, J. Oitmaa, and Z. Weihong, Phys. Rev. B **66**, 054401 (2002).
[19] J. Sirker, Z. Weihong, O. P. Sushkov, and J. Oitmaa, Phys. Rev. B **73**, 184420 (2006).
[20] A. Moreo, E. Dagotto, T. Jolicoeur, and J. Riera, Phys. Rev. B **42**, 6283 (1990).
[21] A. Chubukov, Phys. Rev. B **44**, 392 (1991).
[22] J. Ferrer, Phys. Rev. B **47**, 8769 (1993).
[23] M. Mambrini, A. Läuchli, D. Poilblanc, and F. Mila, Phys. Rev. B **74**, 144422 (2006).
[24] Explicit tabulation of $O_i^n$ is electronically available upon request from the authors.
[25] C. Knetter and G. S. Uhrig, Eur. Phys. J. B **13**, 209 (2000).
[26] F. J. Wegner, Ann. Phys. **506**, 77 (1994).
[27] A graph of length $n$ is composed by $n$ steps. Each step connects a given site with its nearest neighbors along both the $\mathbf{x}, \mathbf{y}$ directions and the diagonals.
[28] J. Oitmaa, C. Hamer, and W. Zheng, *Series Expansion Methods for Strongly Interacting Lattice Models* (Cambridge University Press, UK, 2006).
[29] The explicit expressions of the triplet dispersion $\omega(\mathbf{k})$ and the hopping elements $c_{\mathbf{l}}$ in terms of $J_1$, $J_2$, and $J_3$ are too lengthy to be displayed in written form and will be made available electronically upon request from the authors.
[30] A. Guttmann, in *Phase Transitions and Critical Phenomena*, Vol. 13, edited by C. Domb, and J. L. Lebowitz (Academic, London, 1989).